Orientational order in nitrogen monolayers adsorbed on graphite at low temperature

R. Wang,* S. -K. Wang, H. Taub, and J. C. Newton
Department of Physics and Astronomy, University of Missouri—Columbia, Columbia, Missouri 65211

H. Shechter
Physics Department and Solid State Institute, Technion—Israel Institute of Technology, Haifa 32000, Israel
(Received 24 September 1986)

Elastic neutron diffraction has been used to study the structure of N_2 films adsorbed on the (0001) surfaces of an exfoliated graphite substrate at coverages Θ between 1.0 and 1.67 layers and at temperatures below 11 K. For $\Theta=1.0$, the diffraction patterns can be fit by the in-plane rectangular $\sqrt{3}\times 3$ herringbone structure denoted C (commensurate), previously inferred from low-energy electron diffraction (LEED) experiments. Analysis of the relative Bragg-peak intensities in the neutron diffraction pattern of the C phase extends the LEED results by yielding a value of $\phi=45°\pm 5°$ for the angle between the N—N bond and the short axis of the unit cell. Also, we find a substantially smaller Debye-Waller factor for this phase than previously inferred from x-ray experiments. At coverages $\Theta=1.13$ and 1.27, the diffraction patterns are consistent with the uniaxial incommensurate (UI) phase seen by LEED. The patterns can be fit with the same molecular orientational parameters as for the C phase. We find the compression of the monolayer to be complete at $\Theta=1.67$ where the film density is $\sim 10\%$ greater than for the C phase. Fits to the diffraction pattern at this coverage indicate a slight oblique distortion of the unit cell from hexagonal symmetry. For this nearly triangular incommensurate (TI) phase, we obtain orientational parameters in the ranges $30° < \phi < 45°$ and $10° < \beta < 20°$ where β is the tilt angle of the N—N bond with respect to the surface. At coverages between $\Theta=1.27$ and 1.40, there is evidence of coexistence of the UI and TI phases.

I. INTRODUCTION

Nitrogen adsorbed on graphite provides an interesting system for investigating molecular orientational ordering on surfaces. This simple diatomic molecule has an appreciable quadrupole moment which is believed to play a major role in determining its orientational ordering in condensed phases. The graphite basal plane provides a chemically inert surface with sufficient corrugation to stabilize a commensurate monolayer phase at low coverages but weak enough to allow both partially and completely incommensurate monolayer phases at higher coverages. As reviewed in Ref. 1, three different orientationally ordered monolayer phases have been observed at low temperatures: (1) an in-plane (N—N bond parallel to the surface) rectangular $\sqrt{3}\times 3$ herringbone structure denoted C (commensurate); (2) an in-plane uniaxial incommensurate herringbone structure denoted UI; and (3) the fully compressed monolayer phase which has been called triangular incommensurate (TI).

Orientational ordering in two-dimensional quadrupolar systems has been well studied theoretically. The work is generally of two types. One is mean-field calculations[2] which consider a system of point quadrupoles on a triangular lattice subject to the crystal field of a substrate. These have been very helpful in suggesting types of monolayer structures for interpreting diffraction experiments, e.g., in-plane two-sublattice herringbone, four-sublattice pinwheel, two-sublattice tilted, etc. The other type of calculation has been computer simulations based on detailed modeling of the intermolecular and molecule-substrate interactions. Commensurate,[3–5] incommensurate,[4–7] and bilayer[8] structures of N_2 on graphite have all been studied in this way.

Despite the progress in simulating the different N_2-monolayer phases, there is little direct experimental evidence to support the molecular orientations predicted. To gain perspective on the problem, it is helpful to review briefly some of the experimental investigations of the structure of these phases. A $\sqrt{3}\times\sqrt{3}$ commensurate structure of N_2 on graphite was first found in neutron-diffraction experiments.[9] Since only a single Bragg peak was observed, no determination of the molecular orientation could be made. Subsequent neutron experiments[10] found a second Bragg peak at low temperatures indicating a doubling of the unit cell in at least one direction. This strongly suggested the presence of an orientationally ordered phase. Diehl *et al.*[11] were able to show that systematic extinctions in the low-energy electron diffraction (LEED) pattern of the C phase were consistent with an in-plane two-sublattice herringbone arrangement of the molecules as shown in Fig. 1. Later Diehl and Fain[12] observed a uniaxial compression of the C phase just above completion of the C monolayer. The same extinction arguments led them to conclude that the UI phase also had an in-plane herringbone structure. More recently, You and Fain[13] have interpreted their LEED data on the fully compressed monolayer as a triangular incommensurate "two-out" structure in which the N—N bonds in both sublattices are tilted with respect to the graphite surface. Thus, while there is considerable diffraction data to support the existence of three distinct orientationally ordered

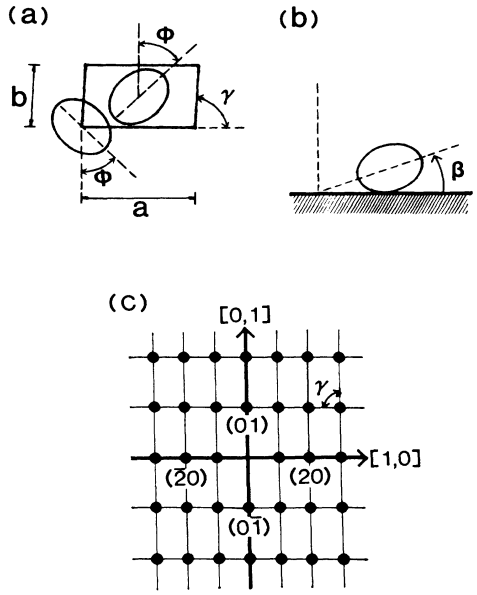

FIG. 1. Definition of structural parameters for a two-sublattice N_2 monolayer: (a) projection of the unit cell on the graphite surface, (b) side view showing tilt of the molecular axis, and (c) two-dimensional reciprocal lattice of the oblique cell in (a).

monolayer phases, the orientational parameters ϕ and β defined in Fig. 1 have not been determined for any of them.

There are several reasons for the difficulty in determining the orientation of the adsorbed N_2 molecule. The LEED experiments[11–13] are hampered by multiple-scattering effects which complicate the interpretation of the diffracted beam intensities. In general, it is not possible to determine the orientation of adsorbed molecules by comparing kinematically calculated structure factors with observed LEED patterns. Unlike LEED, x-ray diffraction is not strongly affected by multiple scattering. However, the molecular form factor attenuates Bragg reflections at large momentum transfer Q. In a recent x-ray study of N_2 adsorbed on exfoliated graphite (Papyex),[14] only two Bragg peaks of the monolayer were observed. The intensity ratio of these two peaks is insufficient to determine ϕ and β.

It is the purpose of this paper to show that neutron diffraction has some advantages over both LEED and x-ray scattering for investigating the orientational order in monolayers of nearly spherical diatomic molecules. As in the case of x rays, the neutron interaction with matter is so weak that the intensities of Bragg reflections can be analyzed by conventional kinematic theory.[15,16] We shall see that scattering from the point nuclei rather than the electron charge cloud allows higher-order Bragg peaks to be observed whose intensities depend sensitively on the molecular orientation. These peaks were not seen in previous neutron studies[9,10] which were confined to $Q<3$ Å^{-1}. As discussed below, their observation is facilitated by the use of a position-sensitive detector with a counting rate several times higher than the single detector used in the earlier experiments.

Our study of the orientational ordering in the three low-temperature monolayer phases of N_2 on graphite is organized as follows. A description of the neutron-diffraction technique and the data-analysis procedure is given in the next section. In Sec. III, we present the observed diffraction patterns and the monolayer structural parameters derived from their analysis. Finally, our results and conclusions are summarized in Sec. IV.

II. EXPERIMENTAL DESCRIPTION

The neutron-diffraction experiments were performed with the two-axis spectrometer equipped with a position-sensitive detector[17] located at port "*D*" of the University of Missouri Research Reactor. The linear detector subtended a scattering angle 2θ of 25° so that with an incident neutron wavelength of 1.29 Å a continuous range of momentum transfers up to $Q=8$ Å^{-1} could be accessed in four successive positions of the detector arm. Data collected is stored in channels of width 0.1°. Counting rates were such that after 12 h in one arm position $\sim 40\times 10^4$ counts could be detected in the highest channel of the {2 0} Bragg peak of the *C*-monolayer phase (background scattering from the bare graphite substrate subtracted).

The sample consisted of 40 disks of an exfoliated graphite (Papyex[18]) having a mass of 51 g. The disks were 3.8 cm in diameter and formed a stack 5-cm high when enclosed in an aluminum sample cell. The Papyex specific surface area was measured to be 21 m^2/g from a vapor-pressure isotherm measurement with N_2 at 78 K. Completion of the *C*-monolayer phase ($\Theta=1.0$) was taken to be at the foot of the substep in the isotherm occurring at a pressure of 5.6 Torr. To the accuracy of our measurement, this coverage definition is the same as in a previous heat-capacity study of monolayer N_2 on graphite.[19] The sample was oriented with the scattering vector **Q** parallel to the foil planes and cooled by a closed-cycle refrigerator. All measurements were performed at temperatures <11 K in order to minimize the effect of the Debye-Waller factor.

The profile analysis technique which we used to fit a model structure factor to the diffraction patterns has been described elsewhere.[16,20] For each of the orientationally ordered phases, the structure factor is calculated explicitly from the nuclear position of each atom in the unit cell. Motion of the nuclei about their equilibrium position is assumed to be small enough that it can be treated by a Debye-Waller factor of the form $\exp(-Q^2\langle u^2\rangle)$ where the mean-square displacement $\langle u^2\rangle$ is taken to be the same for all nuclei. Thus no molecular form factor is introduced to account for the nuclear motion as in the analysis of orientationally disordered phases. The small values of $\langle u^2\rangle \lesssim 0.03$ Å^2 which we have found indicate this to be a reasonable approach.

A line-shape analysis of the diffraction patterns is necessitated by the overlap of Bragg peaks which complicates the separation of their integrated intensities. The overlapping results from the asymmetric Warren line

shape of the peaks,[9] the finite coherence length L of the monolayer diffraction arrays, and the finite Q resolution of the spectrometer. We emphasize that, despite the small L value (~ 100 Å) for our sample compared to graphite single crystals,[21] the relative integrated peak intensities can be determined quite reliably.[20]

III. RESULTS

A. Commensurate phase

The diffraction pattern from a N_2 film at coverage $\Theta = 1.0$ (defined above) is shown in Fig. 2(a) after subtraction of the graphite background. Data is missing from Q regions of intense graphite peaks plotted in Fig. 2(b). The N_2 peak positions can be indexed by the commensurate $\sqrt{3}\times 3$ unit cell found in LEED experiments[11] at the same coverage. The cell parameters are $a = 7.38$ Å, $b = 4.26$ Å, and $\gamma = 90°$ as defined in Fig. 1. Several higher-order Bragg peaks of the monolayer are easily observed. Indeed, two of them, the {4 1} and {3 2}, are more intense than the {2 1} peak[22] which earlier experiments[10] interpreted as the signature of orientational ordering.

We began our fitting of the relative Bragg-peak intensities in the C-phase diffraction pattern by assuming the in-plane [$\beta = 0$ in Fig. 1(b)] herringbone structure inferred by LEED.[11] The herringbone arrangement of the molecules has glide lines parallel to the two lattice vectors **a** and **b**. This symmetry implies the absence of reflections (h 0) and (0 k) with h and k odd in agreement with the diffraction pattern in Fig. 2(a). The reader is referred to Fig. 1(c) for a diagram of the two-dimensional reciprocal lattice. Note that if the molecules were to stand on end [$\beta = 90°$ in Fig. 1(b)] forming a simple $\sqrt{3}\times\sqrt{3}$ lattice, then all of the higher-order reflections with $h + k$ odd would vanish. We now show that for the in-plane structure, the intensity of these peaks is sensitive to the azimuthal orientation of the molecules, ϕ.

In Fig. 3, we have calculated the diffraction profiles for ϕ values of 35°, 45°, and 55° in the Q region from 3.4 to 5.0 Å^{-1}. The profiles have been scaled to give the observed intensity for the {2 0} peak which is the most intense peak in the pattern [see Fig. 2(a)]. Also, the same constant has been added to each profile to account for incoherent scattering from the film.[23] The calculated profiles include a Debye-Waller factor of the form

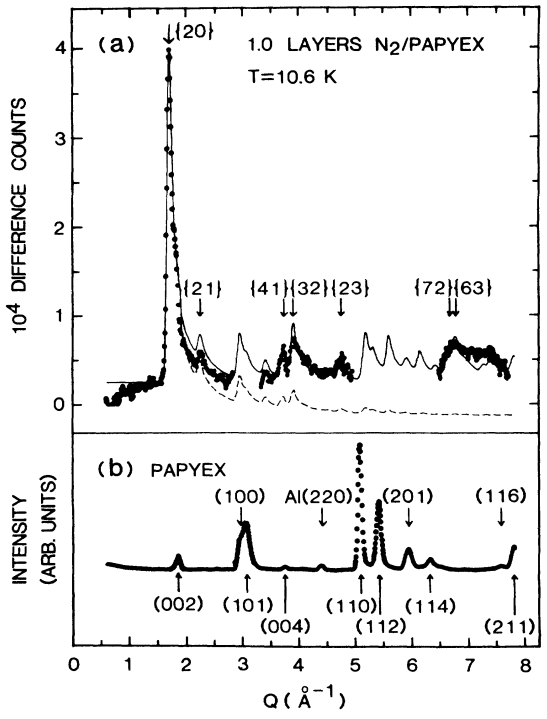

FIG. 2. (a) Neutron diffraction pattern from 1.0 layers of N_2 adsorbed on Papyex at 10.6 K after subtraction of the Papyex background. The solid curve has been calculated for the cell parameters listed in Table I with $\phi = 40°$, $\beta = 0$, $\langle u^2\rangle = 0.01$ Å^2, and coherence length $L = 105$ Å (defined in Ref. 6). Only the most intense {h k} peaks have been labeled. For the dashed curve, all of these parameters remain the same except $\langle u^2\rangle = 0.1$ Å^2 as reported in Ref. 11. To improve the legibility of the dashed curve, the same incoherent background has been used over the entire Q range. (b) Diffraction pattern of the bare Papyex. In addition to the graphite Bragg peaks, the Al(2 2 0) peak from the sample cell can also be seen.

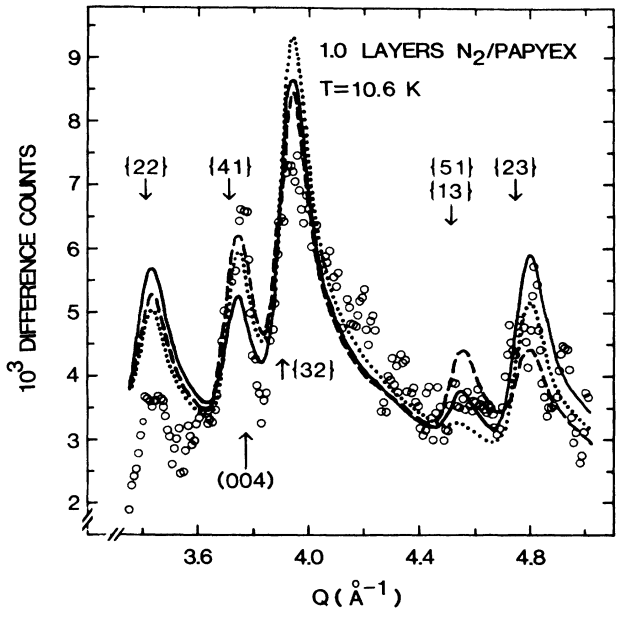

FIG. 3. Detail of the 1.0-layer diffraction pattern of Fig. 1(a) in the Q range most sensitive to the orientational ordering. Profiles have been calculated for various values of the in-plane azimuthal orientation ϕ assuming $\beta = 0$ and $\langle u^2\rangle = 0.01$ Å^2: $\phi = 55°$ (solid curve), $\phi = 45°$ (dotted curve), and $\phi = 35°$ (dashed curve). The difference in the {5 1} and {1 3} peak positions is unresolved. Again, only the most intense {h k} peaks have been labeled.

$\exp(-Q^2\langle u^2\rangle)$ with $\langle u^2\rangle = 0.01$ Å^2. This value of $\langle u^2\rangle$ was chosen to fit the intensity of the {72} and {63} peaks at the highest Q. Due to the relatively small-Q range in Fig. 3, the fit to the peaks in this region is less sensitive to the choice of $\langle u^2\rangle$.

It is clear from Fig. 3 that the calculated diffraction profiles change considerably for a 10° variation of ϕ about 45°. A qualitative comparison of these profiles with the observed pattern allows us to define a range of ϕ which best fits the data. For example, the profile calculated for $\phi = 35°$ predicts the peak containing the {51} and {13} reflections to be the same intensity as the {23} peak while the former is barely visible in the data. For $\phi = 55°$, the {22} peak is stronger than the {41} peak contrary to the observed pattern. Also, $\phi = 55°$ gives the smallest ratio for the {41} to {32} peak intensity in worst agreement with the data.

The intensity of the N_2 peaks in Fig. 3 could be affected by imperfect background subtraction near the graphite (101) and (004) reflections. However, we found the qualitative features of the monolayer pattern in this region to be reproducible in three separate runs in which the graphite background was first measured and then the N_2 loaded. It is possible that interference effects between the film and substrate near the graphite (004) peak could introduce *systematic* errors in the observed monolayer {41} and {32} peak intensities. But generally, we have found the larger interference effects expected near the graphite (002) peak[24] very difficult to reproduce due to electronic instabilities of the position-sensitive detector. Thus, we consider the presence of smaller interference effects near the graphite (004) peak to be unlikely. We conclude that the best fit to the diffraction pattern in Fig. 3 occurs for ϕ values in the range from 40° to 50°. The solid curve in Fig. 2(a) is calculated for $\phi = 40°$.

We have performed several other tests of our fit to the C-phase diffraction pattern. The dashed curve in Fig. 2(a) is calculated for the in-plane herringbone model with $\phi = 40°$ but with a larger value of $\langle u^2\rangle = 0.1$ Å^2 in the Debye-Waller factor as inferred by Morshige *et al.*[14] in their recent x-ray study of the C phase. This larger value of $\langle u^2\rangle$ greatly attenuates the higher-order Bragg reflections so that the height of the {41} and {32} peaks above the incoherent background is about $\frac{1}{3}$ of that observed. Furthermore, the calculated {72} and {63} peaks are predicted to be too weak to be observed. It appears then that the large value of $\langle u^2\rangle$ inferred by these authors is an artifact of their analysis based on only two Bragg peaks. We should point out, however, that the error in our value of $\langle u^2\rangle = 0.01$ may be large. It could be increased to ~ 0.03 Å^2 while ϕ remained within the range quoted above.

We also checked the sensitivity of our fits to tilting the molecule with respect to the surface. For a fixed value of $\phi = 45°$, the angle β could be increased to $\sim 15°$ without a discernible degradation of the fit.

B. Uniaxial compressed phase.

The neutron diffraction patterns at $\Theta = 1.13$ and 1.27 layers shown in Figs. 4 and 5, respectively, are qualitatively similar to that of the C phase in Fig. 2(a). The main differences are that at these higher coverages the peaks are somewhat broader and shifted upward slightly in Q. The LEED results of Diehl and Fain[12] on weakly incommensurate N_2 monolayers suggested fitting these patterns with UI structure.

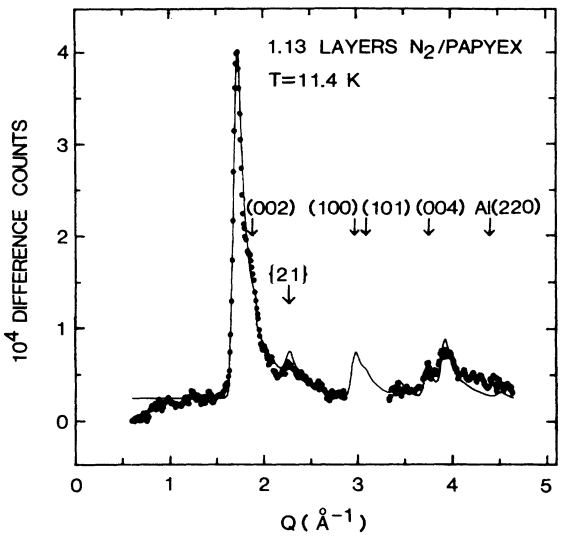

FIG. 4. Neutron diffraction pattern from 1.13 layers of N_2 on Papyex at 11.4 K after subtraction of the Papyex background. The solid curve has been calculated for the cell parameters listed in Table I with $\phi = 40°$, $\beta = 0$, and $\langle u^2\rangle = 0.01$ Å^2.

The solid curve in Fig. 4 has been calculated assuming a UI phase with a unit cell which has been compressed 0.7% along the **a** direction from that of the C phase. The uniaxial compression results in a splitting of the {20}

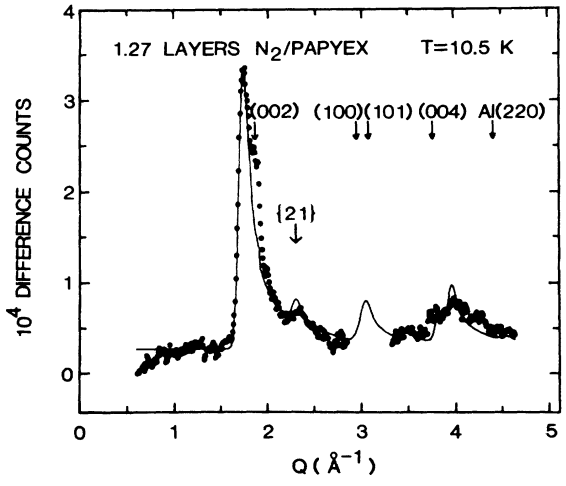

FIG. 5. Neutron diffraction pattern from 1.27 layers of N_2 on Papyex at 10.6 K after subtraction of the Papyex background. The solid curve has been calculated for the cell parameters listed in Table I with $\phi = 40°$, $\beta = 0$, and $\langle u^2\rangle = 0.01$ Å^2.

peak of the C phase into two peaks which are unresolved in the main peak of the pattern near $Q=1.7$ Å^{-1} in Fig. 4. This splitting accounts for part of the increased width observed in the peak's leading edge. The fit could be improved by a further widening of the peak. This was achieved by decreasing the monolayer coherence length from its value of 105 Å in the C phase to 95 Å.

In analyzing the $\theta=1.13$ diffraction pattern, we have assumed the in-plane herringbone structure with the glide-line symmetries inferred for the UI phase by LEED.[12] Although not shown, we calculated profiles for the same range of ϕ values as in Fig. 3. The value of $\langle u^2\rangle$ in the Debye-Waller factor was fixed at 0.01 Å^2. As for the C phase, we find that the best fit occurs in the ϕ range from 40° to 50°. The solid curve in Fig. 4 is calculated for $\phi=40°$ and $\beta=0°$.

To fit the $\theta=1.27$ diffraction pattern in Fig. 5 required a larger uniaxial compression than at $\theta=1.13$. This can be seen more clearly in Fig. 6 where the shift in the main peak position between these two coverages is readily observed. The solid curve in Fig. 5 has been calculated for a lattice parameter $a=7.14$ Å which is 3.3% smaller than for the C phase. This compression completely accounts for the broadening observed in the leading edge of the main peak.[25] It was not necessary to decrease the monolayer coherence length from the value of 95 Å used in the fit at $\theta=1.13$. After performing the same type of analysis as in Fig. 3, we inferred ϕ in the range 40°—50° as before. The solid curve in Fig. 5 is calculated for $\phi=40°$ and $\beta=0$.

For both $\theta=1.13$ and 1.27 coverages, we estimate the same uncertainty in the values of $\langle u^2\rangle$ and the tilt angle β as for the C phase; i.e., $\langle u^2\rangle$ is in the range from 0.01 to 0.03 Å^2 and $\beta<15°$.

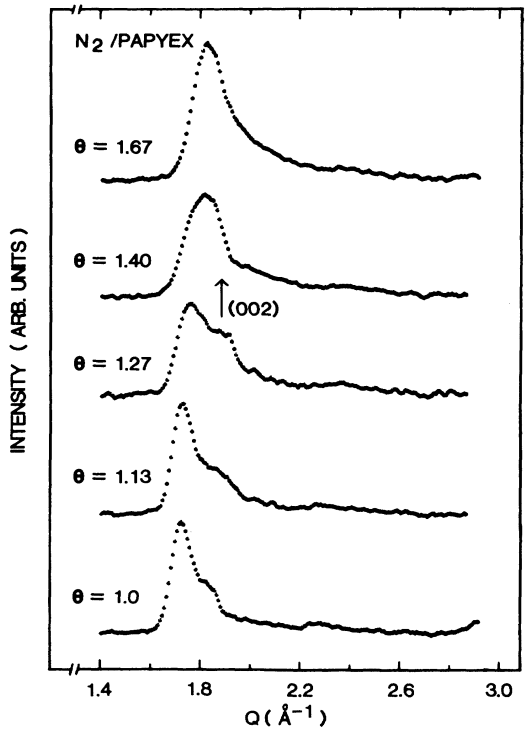

FIG. 6. Coverage dependence of the low-Q portion of the neutron diffraction patterns of N_2 adsorbed on Papyex below 11 K. In each pattern, the substrate scattering has been subtracted.

C. Triangular incommensurate phase

As can be seen in Fig. 6, the main diffraction peak of the film near $Q=1.8$ Å^{-1} continues to broaden between 1.27 and 1.40 layers. A number of attempts were made to analyze the 1.40-layer diffraction pattern as that from a single-monolayer phase but without success. Specifically, we were unable to find an incommensurate unit cell with which we would interpret the line shape of the main peak in terms of a splitting of the (2 0), (1 1), and (1 $\bar{1}$) reflections of the C phase. Among the incommensurate structures considered were rectangular cells either uniaxially or isotropically compressed from the C phase. We also investigated the effect of small oblique distortions of these cells. In no case were we able to fit the peak line shape as well as at lower coverages. For this reason, we have considered the possibility that there are two coexisting monolayer phases contributing to the diffraction pattern at 1.40 layers. We shall discuss this interpretation further in the next section.

The main peak in the diffraction patterns of Fig. 6 narrows between $\theta=1.40$ and 1.67 layers. Measurements at higher coverages showed its width to remain constant up to 2.6 layers.[26] This behavior suggested to us that at 1.67 layers we had reached the fully compressed monolayer phase referred to as "triangular incommensurate" by Fain and co-workers.[1,13]

The full diffraction pattern at 1.67 layers is shown in Fig. 7. We could fit the main peak near $Q=1.8$ Å^{-1} by assuming a hexagonal unit cell with a lattice constant 5.2% smaller than for the C phase. This fit required a further decrease in the monolayer coherence length to 60 Å. With $\langle u^2\rangle$ fixed at 0.1 Å^2, we systematically varied the orientational parameters ϕ and β to obtain the best fit in the Q range from 3.5 to 5 Å^{-1}. We did not require the ϕ and β angles of the two molecules to be the same nor was the center of mass of one of the molecules confined to the cell center. We also investigated the effect of unequal compressions along the **a** and **b** lattice vectors of the commensurate cell (see Fig. 1). The most significant improvement in the fit resulted from a slight oblique distortion of the cell for which the angle $\gamma=88.5°$ in Fig. 1(a).[27] For this nearly TI cell, we obtained values of $\phi=30°$ and $\beta=10°$ for both molecules.

The main problem with this structure is a Bragg peak at $Q=7.1$ Å^{-1} which is predicted to be stronger and narrower than the peak observed. To reduce the intensity of this peak, we tried larger values of $\langle u^2\rangle$ but retained the oblique unit cell. The solid curve in Fig. 7 is the best fit which we obtained. It is calculated for $\langle u^2\rangle=0.03$ Å^2 with orientational parameters $\phi=45°$ and $\beta=20°$ for both molecules.

As a result of the simultaneous variation of ϕ and β, the fits to the $\phi=1.67$ diffraction pattern were more tedi-

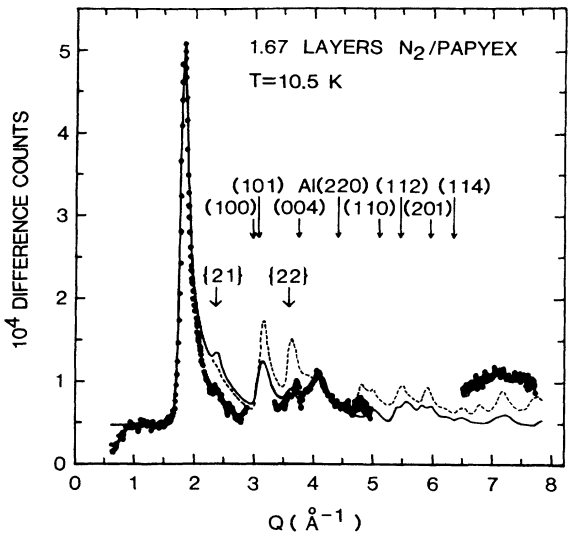

FIG. 7. Neutron diffraction pattern from 1.67 layers of N_2 on Papyex at 10.6 K after the substrate scattering has been subtracted. The solid curve has been calculated for the cell parameters listed in Table I with $\phi=45°$, $\beta=20°$, and $\langle u^2\rangle=0.03$ Å^2. The dashed curve assumes the same cell parameters and $\langle u^2\rangle=0.01$ Å^2 but $\phi=60°$ and $\beta=40°$ as in the model of Ref. 13.

ous and less certain than for the C and UI phases. We consider the difference between the two sets of values obtained for ϕ and β to be representative of their uncertainty. Thus we conclude that for the fully compressed monolayer phase the molecular orientations are in the ranges $30°<\phi<45°$ and $10°<\beta<20°$.

The model just described for the TI phase[28] is similar to the "two-out" structure proposed by You and Fain from LEED experiments.[13] Assuming a hexagonal unit cell and a kinematic approximation in the calculation of the LEED spot intensities, they found molecular orientations in the ranges $50°<\phi<80°$ and $25°<\beta<45°$ to be consistent with their observations.[29] These ranges of ϕ and β lie outside our own. Their best fit was obtained for $\phi=60°$ and $\beta=40°$. The dashed curve in Fig. 7 has been calculated assuming these orientational parameters, our oblique unit cell, and $\langle u^2\rangle=0.01$ Å^2. The fit is worse at the {21} and {22} peaks than for our model (solid curve).[30]

There is theoretical evidence[2,4,31] suggesting that the fully compressed monolayer is unstable to the formation of a four-sublattice pinwheel structure. We have calculated profiles for some pinwheel structures varying the azimuthal orientation ϕ of the three in-plane molecules. None of the profiles fit the $\theta=1.67$ diffraction pattern as well as those for the "two-out" structures.

The profiles which we have compared with the 1.67-layer diffraction pattern have been calculated for a single layer of N_2 molecules. Actually, at this coverage about 30% of the molecules occupy a second layer. This estimate is based on the TI structure having an areal density about 10% greater than for the C phase. Our analysis may still be applicable if the partial second layer is either amorphous or fluid. In this case, we would expect it to contribute broad peaks which would be too weak to be observed. The fact that the diffraction patterns below 11 K do not change between 1.67 and 2.6 layers[26] is consistent with this interpretation of an invisible second layer. Further support comes from our profile calculations for various bilayer structures[26] which indicate an appreciably greater width of the main peak at $Q=1.8$ Å^{-1} than is observed in the $\theta=1.67$ diffraction pattern. Nevertheless, the presence of a partial second layer could still influence the structure of the first layer. In fact, our results suggest that a partial second layer is needed to leave the coexistence region between the UI and TI monolayer phases.

IV. SUMMARY AND CONCLUSIONS

The monolayer structural parameters which we have inferred for each coverage at low temperature are listed in Table I. The ranges given for ϕ and β express our best estimate of the uncertainty in these parameters. Generally, the calculated diffraction profiles are more sensitive to the azimuthal angle ϕ than the tilt angle β for small β. This is because the integrated peak intensity is determined by the projection of the molecule onto the surface.

For the C phase, the values $\phi=44.5°$ and 42.8° calculated in molecular-dynamics (MD) simulations[3,6] and $\phi=44.1°$–$44.9°$ found in ground-state calculations[4] all lie in the experimental range. The value of $\phi=41.0°$ obtained in MD simulations of the UI phase[6] is also within the range which we have found at coverages of 1.13 and 1.27 layers.

At present, we are not aware of any theoretical calculations predicting a "two-out" herringbone structure for the fully compressed N_2 monolayer on graphite. Ground-

TABLE I. Structural parameters as defined in Fig. 1 for the monolayer phases of N_2 adsorbed on Papyex at low temperature (<11 K). All angles are in degrees.

Coverage (layers)	Phase	a (Å)	b (Å)	γ	ϕ	β
1.0	C	7.38	4.26	90	40–50	0–15
1.13	UI	7.33	4.26	90	40–50	0–15
1.27	UI and TI	7.14	4.26	90	40–50	0–15
1.40	UI and TI					
1.67	TI	7.00	4.04	88.5	30–45	10–20

state calculations[31] indicate a pinwheel structure to be more favorable as the monolayer is compressed beyond the UI phase. On the other hand, the LEED experiments of You and Fain[13] support a structure similar to ours, although their best values of the orientational parameters ϕ and β lie outside our ranges at 1.67 layers.

Vernov and Steele[8] have performed MD simulations of N_2 bilayers on graphite. They find that the presence of a second layer results in a flattening of the film so that the molecular axes are more nearly coplanar with the surface ($\beta \rightarrow 0$). It is not clear whether this flattening effect would occur with only a partial second layer. If so, it might explain the absence of a pinwheel structure at 1.67 layers. Vernov and Steele also found for a monolayer undergoing uniaxial compression parallel to the lattice vector **a** [see Fig. 1(a)] that the in-plane azimuthal angle ϕ decreased from 45° to 35° at 0 K. While we do not find such a decrease in ϕ in the UI phases at 1.13 and 1.27 layers, their result is consistent with the range of ϕ values which we find for the TI phase at 1.67 layers. However, the best ϕ values which You and Fain[13] found for the TI phase show the opposite effect—their values tend to be larger than for the C phase.

It would obviously be desirable to reduce the uncertainty in the determination of the orientational parameters ϕ and β. The main limitations of the neutron-diffraction technique are the inherently weak scattering of the film and the imperfect background subtraction near the graphite Bragg peaks. The large counting rates which we have achieved by use of a position-sensitive detector help to overcome the weak scattering problem. Unfortunately, electronic instabilities can result in poor reproducibility of the peak positions so that the quality of the background subtraction can be worse than for a single mechanically positioned detector. A significant improvement in the quality of the diffraction data may be possible by using a system of multidetectors specifically designed for monolayer experiments.

A low-temperature phase diagram of N_2 adsorbed on graphite is shown in Fig. 8. The boundaries of the $C+$UI coexistence region and of the pure UI phase are those inferred by Zhang *et al.*[19] from heat-capacity measurements. The biggest discrepancy between our phase diagram and theirs is the large coexistence region which we find for the UI and TI phases. We have already discussed in Sec. III C the evidence for coexistence of these phases at $\theta = 1.40$. There is also evidence of coexistence at $\theta = 1.27$. In Fig. 5 the fit to the UI structure (solid curve) is poor near the {2 1} peak which appears at the same Q value as in the TI phase. In addition, the shape of the main peak appears distorted (see Fig. 6) between its maximum and the graphite (0 0 2) position. This is the Q range in which the peak maximum occurs in the TI phase. It is interesting to note that the large UI + TI coexistence region indicated in Fig. 8 closely matches the coverage range in which the heat-capacity peak at the orientational disordering transition disappears.[19,32]

The low-temperature phase diagrams of N_2 and ethane[20,33] on graphite bear some resemblance. Ethane

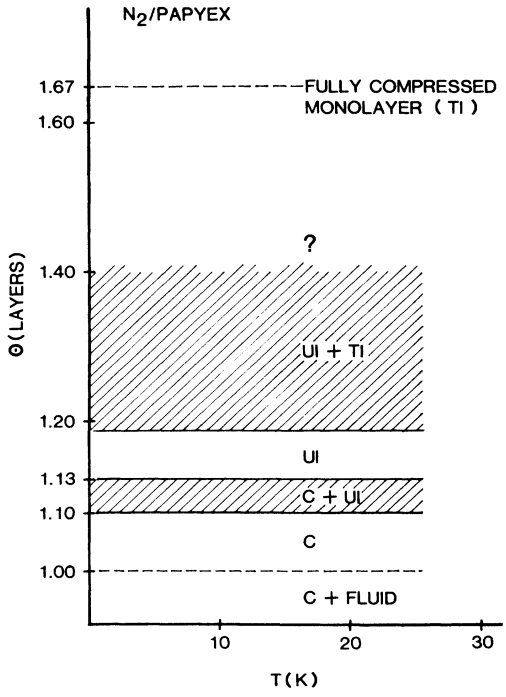

FIG. 8. Low-temperature phase diagram of N_2 adsorbed on the graphite (0 0 0 1) surface. The boundaries of the $C+$UI coexistence region and of the UI phase are from Ref. 31. Although our study has been confined to temperatures below 11 K, we assume the boundaries of the UI + TI coexistence region remain unchanged up to the orientational disordering transition (see Refs. 19 and 32).

(C_2H_6) also has an in-plane commensurate herringbone structure ($S1$) at submonolayer coverages followed by an intermediate phase ($S2$) in a narrow range of coverage near monolayer completion. Between 1.0 and 1.5 layers, the $S2$ phase coexists with a $\sqrt{3}\times\sqrt{3}$ commensurate structure ($S3$) in which the molecules stand on end with the C—C bond perpendicular to the surface. Thus an appreciable amount of second layer is necessary to reach the $S3$ phase. In this respect, it is similar to what we have found for N_2 where the pure TI phase first appears above 1.4 layers. It would be very helpful to have MD simulations of N_2 in this coverage range in order to investigate the role of a partial second layer in stabilizing the fully compressed monolayer phase.

ACKNOWLEDGMENTS

The authors would like to thank S. C. Fain, Jr., L. W. Bruch, W. A. Steele, D. J. Tildesley, R. K. Thomas, and M. H. W. Chan for extensive discussion of our results. This work was supported by National Science Foundation Grant No. DMR-8304366 and Israel-U.S. Binational Science Foundation Grant No. 2687.

*Present address: Bell Laboratories, 1255 S. Cedar Crest Blvd., Allentown, PA 18103.

[1]R. D. Diehl and S. C. Fain, Jr., Surf. Sci. **125**, 116 (1983).

[2]See, e.g., A. B. Harris and A. J. Berlinsky, Can. J. Phys. **57**, 1852 (1979).

[3]J. Talbot, D. J. Tildesley, and W. A. Steele, Mol. Phys. **51**, 1331 (1984).

[4]L. W. Bruch, J. Chem. Phys. **79**, 3148 (1983).

[5]C. Peters and M. L. Klein, Mol. Phys. **54**, 895 (1985).

[6]J. Talbot, D. J. Tildesley, and W. A. Steele, Surf. Sci. **169**, 71 (1986).

[7]C. Peters and M. L. Klein, Phys. Rev. B **32**, 6077 (1985).

[8]A. Vernov and W. A. Steele, Surf. Sci. **171**, 83 (1986).

[9]J. K. Kjems, L. Passell, H. Taub, J. G. Dash, and A. D. Novaco, Phys. Rev. B **13**, 1446 (1976).

[10]J. Eckert, W. D. Ellenson, J. B. Hastings, and L. Passell, Phys. Rev. Lett. **43**, 1329 (1979).

[11]R. D. Diehl, M. F. Toney, and S. C. Fain, Jr., Phys. Rev. Lett. **48**, 177 (1982).

[12]R. D. Diehl and S. C. Fain, Jr., Phys. Rev. B **26**, 4785 (1982).

[13]H. You and S. C. Fain, Jr., Faraday Discuss. Chem. Soc. **81**, 159 (1985).

[14]K. Morishige, C. Mowforth, and R. K. Thomas, Surf. Sci. **151**, 289 (1985).

[15]H. Taub, in *Vibrational Spectroscopies for Adsorbed Species*, edited by A. T. Bell and M. L. Hair, ACS Symposium Series, No. 137 (American Chemical Society, Washington, D. C., 1980), p. 247.

[16]G. J. Trott, H. Taub, F. Y. Hansen, and H. R. Danner, Chem. Phys. Lett. **78**, 504 (1981).

[17]C. W. Tompson, D. F. R. Mildner, M. Mehregany, J. Sudol, R. Berliner, and W. B. Yelon, J. Appl. Cryst. **17**, 385 (1984).

[18]Manufactured by Le Carbone Lorraine, Departement Produits Speciaux, 37 à 41, rue Jean Jaurès, 92231 Gennevilliers, France.

[19]Q. M. Zhang, H. K. Kim, and M. H. W. Chan, Phys. Rev. B **32**, 1820 (1985).

[20]G. J. Trott, Ph.D. thesis, University of Missouri-Columbia, 1981 (unpublished).

[21]K. L. D'Amico, D. E. Moncton, E. D. Specht, R. J. Birgeneau, S. E. Nagler, and P. M. Horn, Phys. Rev. Lett. **53**, 2250 (1984).

[22]In our notation, $\{h\,k\}$ refers to the group of Bragg reflections which are symmetry equivalent and contribute to the same peak in the powder diffraction pattern. The Miller indices h,k are defined by $\mathbf{G}_{hk}=h\,\mathbf{A}+k\,\mathbf{B}$ where $\mathbf{G}_{hk}$ are the two-dimensional reciprocal-lattice vectors [Fig. 1(c)] and **A** and **B** are the primitive vectors of the reciprocal lattice corresponding to the direct lattice vectors **a** and **b**, respectively [Fig. 1(a)].

[23]The additive constant used in the region below $Q=3.0$ Å^{-1} differs from that used at larger Q. This does not present any difficulties in determining the integrated peak intensities.

[24]H. Taub, K. Carneiro, J. K. Kjems, L. Passell, and J. P. McTague, Phys. Rev. B **16**, 4551 (1977).

[25]Imperfect subtraction near the graphite (0 0 2) peak complicates analysis of the trailing edge of the main peak.

[26]S.-K. Wang, J. C. Newton, R. Wang, J. R. Dennison, H. Taub, and H. Shechter (unpublished).

[27]The possibility of a distorted lattice was considered previously in Refs. 1 and 14. However, a specific choice of lattice vectors was not proposed.

[28]To avoid a proliferation of names, we shall continue to refer to the fully compressed monolayer phase as triangular incommensurate following Ref. 1, despite the small oblique distortion which we have found in the unit cell.

[29]Note that the tilt angle β defined in Fig. 1(b) is the complement of the angle θ in Ref. 13.

[30]The intensity of the $\{2\,2\}$ peak does not decrease significantly with $\langle u^2\rangle=0.03$ Å^2 in the Debye-Waller factor.

[31]L. W. Bruch (private communication).

[32]Q. M. Zhang, H. K. Kim, and M. H. W. Chan, Phys. Rev. B **33**, 413 (1986).

[33]J. Suzanne, J. L. Seguin, H. Taub, and J. P. Biberian, Surf. Sci. **125**, 153 (1983).